

A SIMPLE MODEL FOR QUASAR DEMOGRAPHICS

CHARLIE CONROY¹ & MARTIN WHITE^{2,3}

¹Department of Astronomy & Astrophysics, University of California, Santa Cruz, CA, 95060, USA

²Departments of Physics and Astronomy, University of California, Berkeley, CA 94720, USA

³Physics Division, Lawrence Berkeley National Laboratory, Berkeley, CA 94720, USA

Submitted to ApJ

ABSTRACT

We present a simple model for the relationship between quasars, galaxies, and dark matter halos from $0 < z < 5$. In the model, black hole (BH) mass is linearly related to galaxy mass, and galaxies are connected to dark matter halos via empirically constrained relations. A simple “scattered” light bulb model for quasars is adopted, wherein BHs shine at a fixed fraction of the Eddington luminosity during accretion episodes, and Eddington ratios are drawn from a lognormal distribution that is redshift-independent. This model has two free, physically meaningful parameters at each redshift, the normalization of the $M_{\text{BH}} - M_{\text{gal}}$ relation and the quasar duty cycle; these parameters are fit to the observed quasar luminosity function (LF) over the interval $0.5 < z < 4.75$. This simple model provides an excellent fit to the LF at all epochs, and also successfully predicts the observed projected two-point correlation of quasars from $0.5 < z < 2.5$. It is significant that a *single* quasar duty cycle at each redshift is capable of reproducing the extant observations. The data are therefore consistent with a scenario wherein quasars are equally likely to exist in galaxies, and therefore dark matter halos, over a wide range in masses. The knee in the quasar LF is a reflection of the knee in the stellar mass-halo mass relation. The normalization of the $M_{\text{BH}} - M_{\text{gal}}$ relation increases as $(1+z)^2$, consistent with observations, although in our model the normalization is degenerate with the mean Eddington ratio. Future constraints on the quasar LF and quasar clustering at high redshift will provide strong constraints on the model. A further implication of our model is that the autocorrelation function of quasars becomes a strong function of luminosity only at the very highest luminosities, and will be difficult to observe because such quasars are so rare. Cross-correlation techniques may provide useful constraints on the bias of such rare objects. The simplicity of our model allows for rapid generation of quasar mock catalogs from N-body simulations that match the observed luminosity function and clustering to high redshift.

Subject headings: quasars: general — galaxies: evolution — galaxies: high-redshift

1. INTRODUCTION

Quasars are among the most luminous astrophysical objects, and are believed to be powered by accretion onto supermassive black holes (e.g. Salpeter 1964; Lynden-Bell 1969). They have become a key element in our current paradigm of galaxy evolution (e.g., Springel et al. 2005; Croton et al. 2006; Hopkins et al. 2008), and essentially all spheroidal systems at present harbor massive black holes (Kormendy & Richstone 1995), the masses of which are correlated with many properties of their host systems. Despite their importance, and intense theoretical activity, a full theory of the coevolution of galaxies and quasar eludes us.

The current paradigm assumes that every galaxy initially forms in a gas-rich, rotationally-supported system. Once the dark matter halo grows to a critical scale some event, most likely a major merger (Carlberg 1990; Haiman & Loeb 1998; Cattaneo, Haehnelt & Rees 1999; Kauffmann & Haehnelt 2000; Springel et al. 2005; Hopkins et al. 2006, 2008) or instability in a cold-stream fed disk (Ciotti & Ostriker 1997, 2001; Di Matteo et al. 2012), triggers a period of rapid, obscured star formation, the generation of a stellar bulge and a growing black hole (BH). Eventually the accreting BH becomes visible as a quasar, and soon after the star formation is quenched on a short timescale, perhaps via radiative or mechanical feedback from the BH (e.g. Silk & Rees 1998; King 2003; Wyithe & Loeb 2003; Shankar 2009; Natarajan 2012; Alexander & Hickox 2012). Understanding the details of this picture remains an active area of

research.

Phenomenological models for quasar demographics often adopt power-law relations between quasars, galaxies, and dark matter halos (e.g., Efstathiou & Rees 1988; Carlberg 1990; Wyithe & Loeb 2002, 2003; Haiman, Ciotti & Ostriker 2004; Marulli et al. 2006; Lidz et al. 2006; Croton 2009; Shen 2009; Booth & Schaye 2010). In these models, the duty cycle of quasars is tuned to match the observations, and a generic conclusion is that the duty cycle is a strong function of halo mass or quasar luminosity, peaking at a halo mass of $10^{12-13} M_{\odot}$. However, these previous models do not incorporate constraints provided by the galaxy stellar mass function over the interval $0 < z < 5$. And yet, a variety of lines of evidence suggest that the relation between halos and galaxies is highly non-linear, with a characteristic peak in galaxy formation efficiency at a halo mass of $\sim 10^{12} M_{\odot}$ (van den Bosch et al. 2003; Vale & Ostriker 2004; Mandelbaum et al. 2006; Conroy & Wechsler 2009; Moster et al. 2010; Trujillo-Gomez et al. 2011; Behroozi, Wechsler & Conroy 2012). The aim of this paper is to incorporate empirically constrained relations between galaxies and halos into a simple model for quasar demographics. We will demonstrate that a model constructed to match the observed galaxy stellar mass function implies a quasar duty cycle that is independent of galaxy and halo mass at each redshift. This has important implications for physical models aimed at understanding the triggering of quasars and their connection to the evolution of galaxies.

The outline of the paper is as follows. In §2 we describe the model, in §3 the model is compared to data, and a discussion is presented in §4. We conclude in §5. Where necessary we adopt a Λ CDM cosmological model with $\Omega_m = 0.28$, $\Omega_\Lambda = 0.72$ and $\sigma_8 = 0.8$. Unless the h dependence is explicitly specified or parametrized, we assume $h = 0.7$. Dark matter halo masses are quoted as M_{vir} (Bryan & Norman 1998). Luminosities are quoted in Watts and magnitudes in the AB system, and stellar masses assume a Chabrier (2003) stellar initial mass function.

2. THE MODEL

Our goal is to construct a simple model that relates galaxies, quasars, and dark matter halos over the redshift interval $0 < z < 5$. A small number of free parameters will characterize the model, and these parameters will be constrained against observations.

We begin by specifying a dark matter halo mass function and its evolution to $z = 5$. We adopt the fitting functions of Tinker et al. (2008, 2010) for the halo mass function and large-scale bias, which represent the latest fits to these parameters from cosmological N -body simulations. Note that here and throughout we consider only parent halos; satellite halos, also known as subhalos, or not included in the present study. This is a reasonable approximation at high redshift, as quasars inhabit highly biased halos on the steeply falling tail of the mass function and any satellite galaxies of the same mass would live in even more massive halos which are exponentially rare. This assumption will break down at lower luminosities, where the satellite fraction can be expected to rise. This assumption will also fail to account for the small-scale clustering of quasars, in particular the clustering within the halo scale of $\lesssim 1$ Mpc. When we compare to clustering measurements in §3.2 we will therefore restrict our comparison to $R > 1$ Mpc, which is where most of the data lie.

Next, we adopt empirically constrained relations between galaxy stellar mass and dark matter halo mass over the interval $0 < z < 5$ from Behroozi, Wechsler & Conroy (2012). These relations were constrained against the observed galaxy stellar mass function and galaxy star formation rates from $z = 0$ to $z = 8$. The resulting stellar mass-halo mass ($M_{\text{gal}} - M_h$) relation agrees with results obtained from other techniques, including abundance matching, halo occupation models, satellite kinematics, and gravitational lensing (see Behroozi, Wechsler & Conroy 2012). We also adopt an amount of scatter between galaxy mass and halo mass as a function of redshift implied by the model of Behroozi, Wechsler & Conroy (2012). This scatter increases from ≈ 0.2 dex at $z = 0.5$ to ≈ 0.4 dex at $z = 4$.

Galaxies are assigned BHs via the following equation:

$$\frac{M_{\text{BH}}}{10^{10} M_\odot} = 10^\alpha (1+z)^2 \left(\frac{M_{\text{gal}}}{10^{10} M_\odot} \right)^\beta, \quad (1)$$

where M_{gal} and M_{BH} are the stellar mass of the galaxy and mass of the BH, respectively. The available data at $z \sim 0$ is consistent with a linear relation between M_{gal} and M_{BH} , (i.e. $\beta = 1$) which is what we adopt herein, with a normalization constant of $\alpha \approx -3.1$ (Haring & Rix 2004). The scaling with redshift is motivated by observations (McLure et al. 2006; Targett, Dunlop & McLure 2012), but since we fit for α at each redshift, any deviation from $(1+z)^2$ will be absorbed in the redshift-dependence of the parameter α . We adopt a scatter in this relation of 0.3 dex, independent of mass, con-

sistent with the observed scatter in the local $M_{\text{BH}} - \sigma$ relation (Tremaine et al. 2002).

We have chosen to relate M_{BH} to the total stellar mass of the galaxy, rather than specifically to the bulge component. Obviously for bulge-dominated galaxies the distinction is irrelevant, but the differences can grow as we include galaxies with a large disk component. Assuming that bulge properties are the dominant factor in determining M_{BH} , a more refined model would include the evolution and mass-dependence of the bulge-to-total ratio. However for now we neglect this distinction. We do find that our results are relatively robust to modest changes in the slope of the $M_{\text{BH}} - M_{\text{gal}}$ relation (see §3) — and any overall normalization change can be absorbed into our parameter α — so there are reasons to believe a more complex model would achieve a similar level of success in fitting the observations.

In addition to the strong observed correlation between M_{gal} and M_{BH} , there are well-known correlations between M_{BH} and other parameters of the galaxy including the velocity dispersion, σ , and galaxy size, R_e . In fact, Hopkins et al. (2007b) argued for the existence of a BH fundamental plane (relating M_{BH} , σ , and R_e) that has smaller scatter than any other relationship between M_{BH} and a single galaxy property. Another option would therefore have been to connect BHs to galaxies via σ , as for example done by Croton (2009), or via the BH fundamental plane. We choose to use M_{gal} herein because this quantity is readily available for galaxies to $z = 5$, and because the redshift-dependent connection between galaxies and halos is presently available for galaxy stellar masses, but not for galaxy velocity dispersions.

The BH mass is converted to a bolometric quasar luminosity using an Eddington ratio, $L/L_{\text{Edd}} \equiv \eta$, that is independent of redshift:

$$L_Q = 3.3 \times 10^4 \eta \frac{M_{\text{BH}}}{M_\odot} L_\odot. \quad (2)$$

We draw η from a lognormal distribution with mean of $\eta = 0.1$ and a dispersion of 0.3 dex, in agreement with observations (Kollmeier et al. 2006; Shen et al. 2008). In our model the value of the Eddington ratio is degenerate with the normalization of the $M_{\text{BH}} - M_{\text{gal}}$ relation and any intrinsic width in the Eddington ratio distribution is degenerate with scatter in the $M_{\text{BH}} - M_{\text{gal}}$ relation.

In order to compare to observations, we must translate L_Q into magnitudes in a given filter. We adopt the relation between bolometric luminosity and i -band magnitude (k -corrected to $z = 2$) using the relation from Shen et al. (2009):

$$M_i(z=2) = 72.5 - 2.5 \log L_Q \quad (3)$$

$$= -5.26 - 2.5 \log(\eta M_{\text{BH}}) \quad (4)$$

$$= -30.3 - 2.5 (\log \eta + \alpha) - 5 \log(1+z) - 2.5 \beta \log(M_{\text{gal}}/10^{10} M_\odot), \quad (5)$$

where L_Q is in Watts and M_{BH} is in solar masses. The last two relations follow directly from Equations 1 and 2; we include them here to make explicit the connection between M_{gal} and observed quasar magnitude, and also to emphasize the fact that η and α are perfectly degenerate in our model. There is scatter in L_Q at fixed M_{gal} which arises from a combination of scatter in $M_{\text{BH}} - M_{\text{gal}}$ and $L_Q - M_{\text{BH}}$. Assuming 0.3 dex scatter in each relation and adding them in quadrature we obtain a 0.42 dex scatter in L_Q at fixed M_{gal} .

There are two free parameters in this model at each redshift: the normalization of the $M_{\text{BH}} - M_{\text{gal}}$ relation, specified by α ,

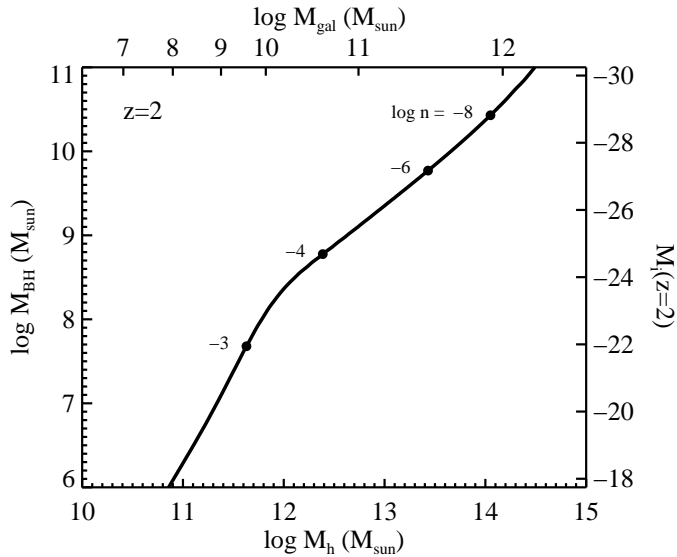


Figure 1. Summary of the model relations at $z = 2$. The quasar LF determines the abundance (see the points on the curve, which label space densities in units of $\log \text{Mpc}^{-3}$) of quasars at a given luminosity (right vertical axis) or BH mass (left vertical axis). For an assumed lifetime, t_Q , this maps to an abundance of galaxies and the stellar mass function provides the appropriate galaxy stellar mass (upper horizontal axis). The empirically constrained $M_{\text{gal}} - M_h$ relations from Behroozi, Wechsler & Conroy (2012) allow us to map this into a halo mass (lower horizontal axis). The curve shown is at $z = 2$, though the general behavior is similar at other redshifts with a steep low-mass slope and a shallower high mass slope (see Figure 8). Note the lower horizontal axis determines the clustering amplitude at fixed redshift while the left vertical axis determines the quasar luminosity.

and the quasar duty cycle, f_{on} . An important, and novel feature of this model is that we adopt a constant duty cycle, independent of luminosity, M_{BH} or M_h . Sometimes the duty cycle is recast into a “lifetime” using the Hubble time: $t_Q \equiv f_{\text{on}} t_H$. As we will demonstrate in the following section, both of these parameters are highly constrained by the observed quasar LF.

The resulting relations between galaxies, halos, and quasars are illustrated in Figure 1. These relations represent the best-fit model constrained by the quasar LF at $z = 2$ (see §3.1). The quasar LF allows us to relate luminosity to number density. For an assumed duty cycle we then have the abundance of BHs of that mass. Similarly the stellar mass function maps galaxy mass to abundance. Thus at fixed duty cycle we obtain a tight constraint on $M_{\text{BH}} - M_{\text{gal}}$. As the stellar mass function and quasar LF contain significant curvature only one combination of normalization and duty-cycle provides a good fit to the data for a range of luminosities (unless we allow significant variation in the lifetime as a function of luminosity).

Figure 2 shows how the predicted quasar luminosity function in our model (at $z = 2$) depends upon several parameters in the model. The amount of scatter in the $L_Q - M_{\text{gal}}$ relation is important for the shape at high luminosity, and indeed the abundance of luminous quasars provides a lower limit on the scatter for any model which places quasars in halos on the exponentially falling part of the mass function. We see that a model with no scatter in the $M_{\text{BH}} - M_{\text{gal}}$ relation predicts drastically fewer bright quasars than a model including scatter (see also White, Martini & Cohn 2008; Shankar, Weinberg & Shen 2010; De Graf et al. 2011; Trainor & Steidel 2012, for related discussion). Variations in the BH mass at fixed galaxy mass (α) change both the normalization and shape of the luminosity function while variation in

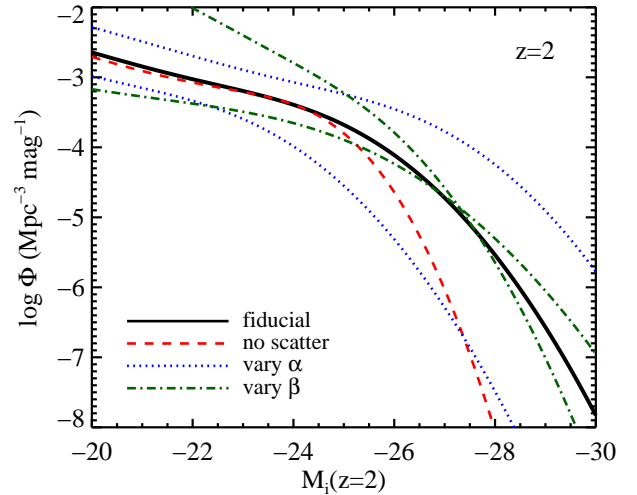


Figure 2. Variation in the predicted luminosity function of quasars at $z = 2$ as a function of the parameters in our model. The dashed (red) line shows how the inclusion of scatter in the $M_{\text{BH}} - M_{\text{gal}}$ relation is important at the high mass end, with models including more scatter predicting more luminous quasars. Variations due to changes in the normalization of the $M_{\text{BH}} - M_{\text{gal}}$ relation ($-3.4 < \alpha < -2.8$; Equation 1) are shown by the dotted (blue) lines, and we see this parameter changes both the normalization and shape of the LF since the galaxy stellar mass function has a particular shape. Finally the dot-dashed (green) line shows variation in the logarithmic slope of the $M_{\text{BH}} - M_{\text{gal}}$ relation ($0.5 < \beta < 1.5$; Equation 1).

the slope of the relation (β) has a large effect on the shape of the LF both at low and high luminosity.

3. COMPARISON WITH OBSERVATIONAL DATA

3.1. The Quasar Luminosity Function

Figure 3 shows the predictions of our model compared to a compilation of observational data from Wolf et al. (2003, COMBO-17; open squares), Richards et al. (2006, SDSS; solid circles), Croom et al. (2009, 2SLAQ+SDSS; open diamonds), Glikman et al. (2010, NDWFS+DLS; stars), and Masters et al. (2012, COSMOS; crosses). We have adopted the following transformation between filters (Wolf et al. 2003; Richards et al. 2006; Croom et al. 2009):

$$M_i(z = 2) = M_g(z = 2) - 0.25 \quad (6)$$

$$= M_{1450} - 0.29 \quad (7)$$

$$= M_{b_j} - 0.71 \quad (8)$$

in order to convert all of the measurements to the $M_i(z = 2)$ system for comparison.

The lifetime, t_Q , and normalization of the $M_{\text{BH}} - M_h$ relation (α in Equation 1) have been fit to the data at each redshift. The grey shaded regions mark the one sigma range of allowed models. In most panels the formal errors are so small that the grey band is buried behind the best-fit relation. The constraints on the parameters are so strong because the data at $z < 4$ samples luminosities both above and below the knee in the LF and because the formal errors on the LF are small.

For comparison we also show the luminosity function that results from assuming a power-law relation between quasar luminosity and halo mass, as has been assumed in many early works (e.g. Efstathiou & Rees 1988; Carlberg 1990; Wyithe & Loeb 2002, 2003; Haiman, Ciotti & Ostriker 2004; Marulli et al. 2006; Lidz et al. 2006; Croton 2009; Shen 2009;

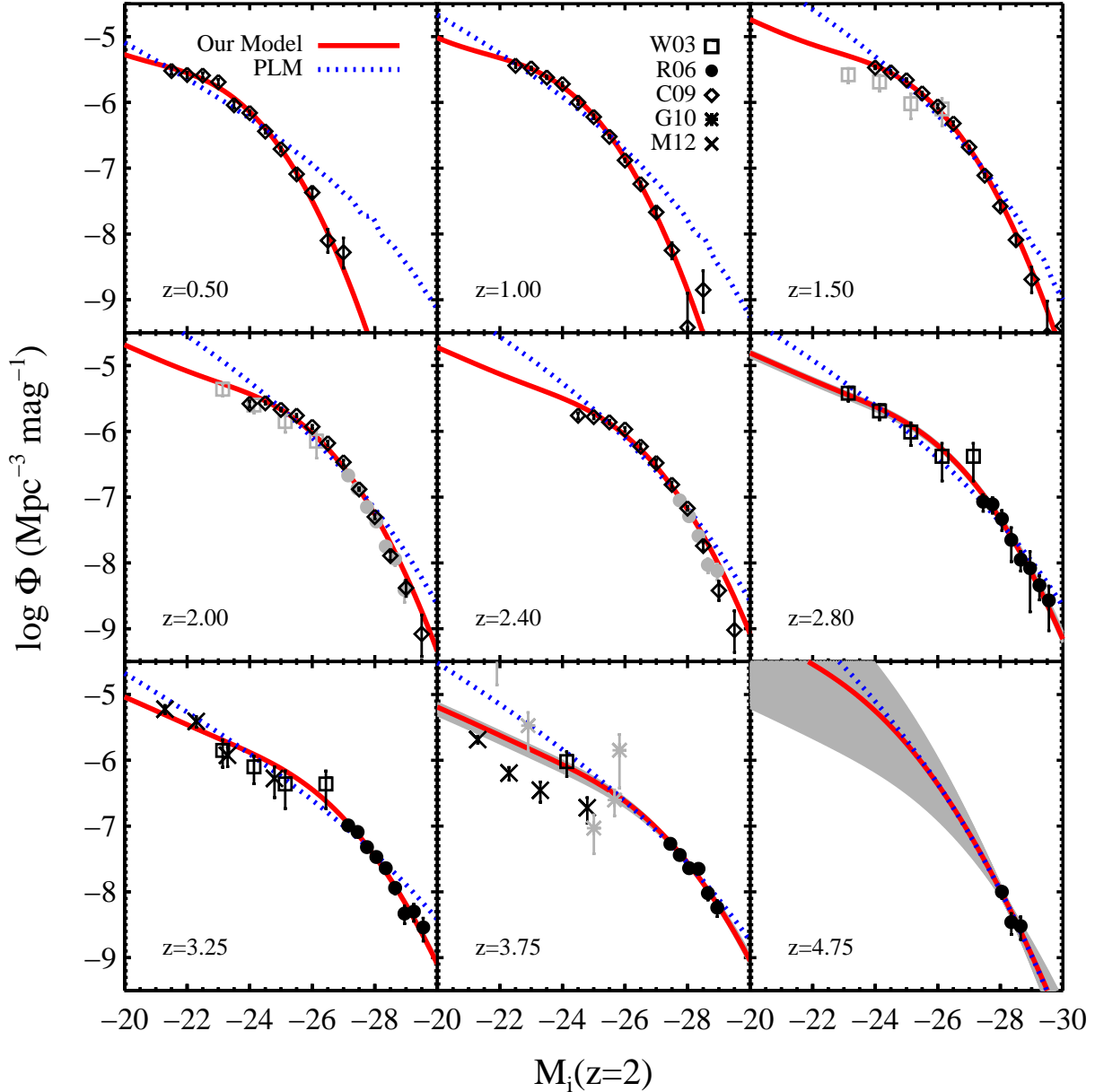


Figure 3. The luminosity function of (active) quasars predicted by our model at different redshifts, as compared to the observations and a simple model in which quasar luminosity is tied to halo, not galaxy, mass (denoted PLM for power-law model). The data are from Wolf et al. (2003, COMBO-17; open squares), Richards et al. (2006, SDSS; solid circles), Croon et al. (2009, 2SLAQ+SDSS; open diamonds), Glikman et al. (2010, NDWFS+DLS; stars), and Masters et al. (2012, COSMOS; crosses). The lifetime, t_Q , and the $M_{\text{BH}}-M_{\text{gal}}$ normalization, α , are fit in each panel and the grey region illustrates the 1σ uncertainty in the model prediction. Only black symbols are included in the fits; the grey symbols generally represent data of lower quality and are included for comparison purposes only.

Booth & Schaye 2010). This model is also characterized by two free parameters, the duty cycle and the normalization of the (power-law) relation between quasar luminosity and halo mass¹. The fundamental difference between our model’s predictions and these power-law models is that we explicitly take into account the efficiency of galaxy formation as a function of mass and redshift (see Figure 1). The two models differ less significantly at higher redshifts for reasons to be discussed below.

¹ The particular model we consider is $L_Q = \gamma M_h^{1.4}$, where γ is the free normalization and the index, 1.4, was chosen from the power-law model of Croton (2009).

In Figure 4 we show the two derived parameters in our model, the quasar lifetime, t_Q (or, equivalently, the duty cycle), and the normalization of the $M_{\text{BH}}-M_{\text{gal}}$ relation, α . In the top panel of Figure 4 we include lines of constant duty cycles of 10^{-2} and 10^{-3} . For reference, the Salpeter time is the e-folding time for a BH growing at a fraction η of the Eddington luminosity with a radiative efficiency of ϵ and is defined as $t_{\text{Salp}} = 4 \times 10^8 (\epsilon/\eta) \text{ yr}$. It is striking how little t_Q varies from $0.5 < z < 3$. The evidence for a decrease in t_Q at $z > 3$ should be regarded as tentative, as the data used to constrain these parameters becomes rather uncertain and is compiled from heterogeneous sources. Our estimates of t_Q are in good

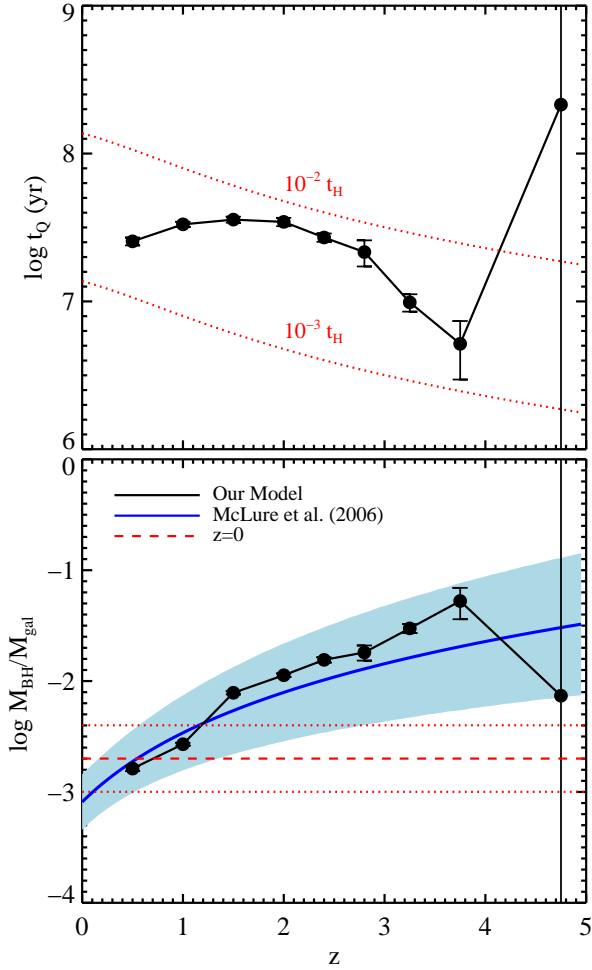


Figure 4. Upper Panel: The duty-cycle, or quasar lifetime, as a function of redshift. We define $t_Q = f_{\text{on}} t_H$ where t_H is the Hubble time at redshift z and f_{on} is the probability that a BH is a luminous quasar (which is independent of luminosity in our model). Also shown are lines of constant $f_{\text{on}} = 10^{-2}$ and 10^{-3} . Lower Panel: The evolution of the normalization of the $M_{\text{BH}} - M_{\text{gal}}$ relation in our model (solid points) compared to a representative sample of results from the literature (see text for further discussion).

agreement with quasar lifetimes inferred by other methods, as summarized in Martini (2004).

In the bottom panel of Figure 4 we show the evolution of the normalization of the $M_{\text{BH}} - M_{\text{gal}}$ relation as inferred from our model. In this panel we also include the normalization measured at $z \sim 0$ (Haring & Rix 2004), and estimates of its evolution in samples of massive galaxies to $z \sim 2$ (McLure et al. 2006). Our model implies an increase in the normalization by roughly an order of magnitude by $z \sim 2-3$, which is in good agreement with a variety of observational constraints to $z \sim 6$ (Peng et al. 2006; Merloni et al. 2010; Decarli et al. 2010; Targett, Dunlop & McLure 2012). Among recent models, we are in good agreement with the models of Hopkins et al. (2007a) and Croton et al. (2006), which predict roughly an order of magnitude increase in M_{BH} at $M_{\text{gal}} \sim 10^{10}$ between $z = 0$ and $z = 3$. In contrast, the simulations of Sijacki et al. (2007) and the semi-analytic model of Fanidakis et al. (2012) predict almost no evolution at the massive end, in conflict with both our model and the data.

Figure 5 shows the model LFs at $z = 0.5$ and $z = 2.4$. Here

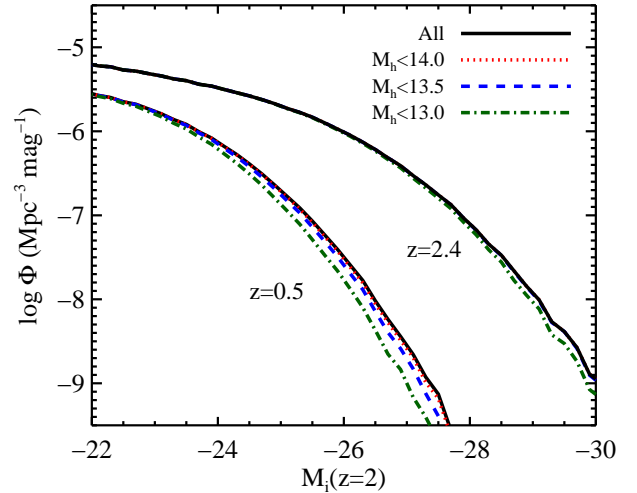


Figure 5. Contribution to the quasar LF from quasars in different halo masses. The curves represent the model LF computed including halos less massive than the values shown in the legend (in units of $\log M_{\odot}$). The model LF is almost entirely insensitive to the presence or absence of quasars in halos more massive than $10^{13.5} M_{\odot}$.

we consider the contribution to the total LF from quasars in halos of different masses. Specifically, we construct model LFs by selecting quasars residing in halos less massive than $\log(M_h/M_{\odot}) < 13.0, 13.5,$ and 14.0 . The purpose of this figure is to demonstrate that massive halos contribute very little to the total LF. In fact, the model is almost entirely insensitive to what happens in halos more massive than $\log(M_h/M_{\odot}) < 13.5$, owing to their rarity relative to lower mass halos. This has important consequences for any model that is tuned to match the quasar LF, as we discuss in §4.

In Figure 3 we adopted our fiducial values for the slope and scatter in the $M_{\text{BH}} - M_{\text{gal}}$ and $L_Q - M_{\text{BH}}$ relations. We found that we can find equally good fits if we adjust the scatter in the $L_Q - M_{\text{gal}}$ relation between 0.3 and 0.6 dex, if we modify the slope of the $M_{\text{BH}} - M_{\text{gal}}$ relation to $\beta = 4/3$ or $5/3$, or even if we change the overall normalization in the $M_{\text{gal}} - M_h$ relation. These changes result in different best-fit values for t_Q and α . Similarly, since α and η are perfectly degenerate in our model we can find very good fits if the Eddington ratio is allowed to vary, although large changes in η lead to disagreement with the more direct measures of the $M_{\text{BH}} - M_{\text{gal}}$ relation shown in Figure 4. Future constraints on the $M_{\text{BH}} - M_{\text{gal}}$ relation as a function of redshift will, in the context of our model, provide strong constraints on the evolution of the scatter and the mean Eddington ratio.

3.2. Quasar Clustering

With the model parameters constrained by the quasar LF, we are now able to make predictions for the clustering of quasars as a function of luminosity and redshift. Recall that our model is characterized by two parameters, the quasar lifetime, t_Q , and the normalization of the $M_{\text{BH}} - M_h$ relation, α . In the model, we assume that quasars are a random sample of the BHs in halos, and therefore t_Q has no effect on the clustering of quasars. The clustering is therefore only sensitive to α , and this parameter is well-constrained at $z < 4$ (see Figure 4). Moreover, α has an increasingly minor effect on the predicted clustering at higher redshifts.

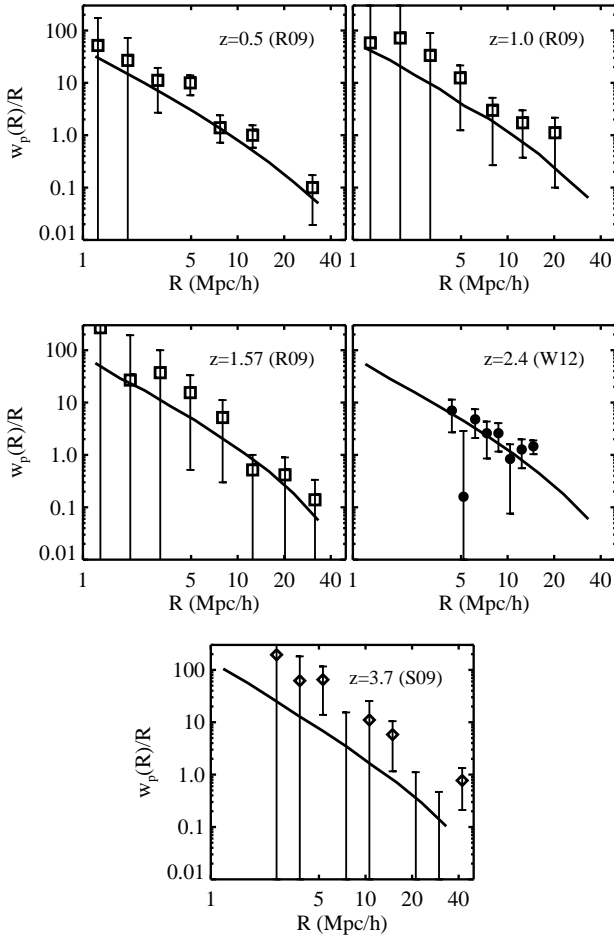


Figure 6. The projected correlation function, $w_p(R)$, vs. projected distance, R , at 5 redshifts chosen to be representative of the data. We include results from Ross et al. (2009, R09), White et al. (2012, W12), and Shen et al. (2009, S09), all of which are based on data from the Sloan Digital Sky Survey. At the highest redshift there is some tension between the model and data, but the error bars are large and the simulation box is too small to provide model predictions at the largest scales. Future measurements of the clustering of both low and high redshift quasars will provide powerful constraints on the model.

Figure 6 shows a comparison of our model and the data on the projected autocorrelation function, $w_p(R)$, as a function of projected (comoving) distance, R , for a variety of redshifts chosen to illustrate the current constraints. We have computed the model correlation function by populating the halos drawn from an N-body simulation² with BHs using the best-fitting relations derived above, and then calculating the clustering of BHs within the luminosity range of each observational sample. This allows us to take into account the scale-dependent

² The simulation employed 2048³ particles in a cubic box of side length 1 Gpc with a force softening of 14kpc (comoving) and was run with the TreePM code of White (2002). Halos were found with a friends-of-friends algorithm (Davis et al. 1985) with a linking length of 0.168 times the mean inter-particle spacing. Spherical over-density masses were computed for each halo (including a correction for finite resolution). For the range of halo masses and redshifts of interest, masses defined via $180\times$ the background density are almost identical to the ‘virial’ definition employed by Behroozi, Wechsler & Conroy (2012)

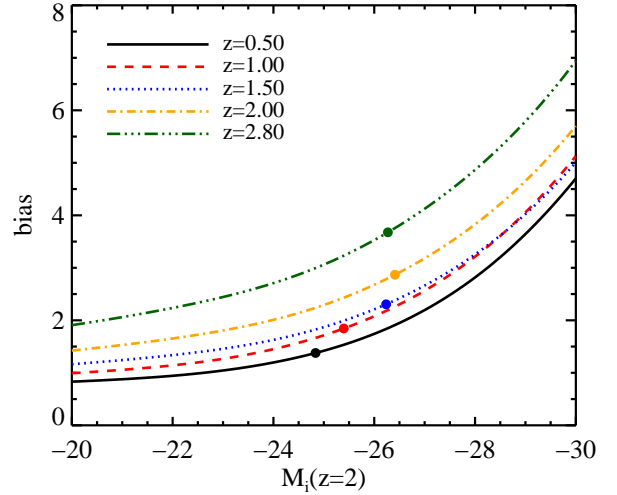


Figure 7. The large-scale bias predicted by our model as a function of luminosity due to the steepness of the $M_{\text{BH}} - M_h$ relation at low mass (see Figure 8). The steepness of the relation at high luminosity depends on the scatter in the model, being less steep for more scatter. We have marked on the curves where the quasar number density is $5 \times 10^{-7} \text{Mpc}^{-3}$, which corresponds to of order 100 quasar pairs within 20Mpc in a survey volume of 10^{10}Mpc^3 . To accurately measure the bias of objects at lower space densities one would need to resort to cross-correlations.

bias and non-linearities, which are important on Mpc scales.

We have populated the halos in the simulation at random, neglecting any properties of the halos apart from their mass (e.g., whether they have had a recent major merger). The majority of models assume that quasar activity occurs due to the major merger of two gas-rich galaxies, since this scenario provides the rapid and violent event needed to funnel fuel to the center of the galaxy (e.g. via the bars-within-bars instability; Shlosman et al. 1989) and feed the central engine while at the same time giving a connection between black hole fueling and the growth of a spheroidal stellar component (e.g., Hopkins et al. 2008). If black hole growth is feedback limited, it is only a rapidly growing potential well that can host a rapidly accreting BH.

Fortunately for such theories, the probability that a halo will undergo a major merger in a short redshift interval is only weakly dependent on the mass of the halo (Lacey & Cole 1993; Percival et al. 2003; Cohn & White 2005; Wetzel, Cohn & White 2009; Fakhouri & Ma 2009; Hopkins et al. 2010b), i.e., the mass function of such halos is almost proportional to the mass function of the parent population. Similarly the clustering properties of recently merged halos are similar to a random sample of the population with the same mass distribution (Percival et al. 2003; Wetzel, Cohn & White 2009). Thus in any redshift interval the fraction of halos of mass M_h that undergo a quasar event is almost independent of M_h and z and can be regarded as a random selection.

The agreement between the data and the model is excellent at $z < 3$, especially considering that the model was only tuned to the quasar LF. The model under-predicts the clustering at $z \sim 3.7$, although the errors on the data are large. This model prediction is quite robust: the $M_{\text{BH}} - M_{\text{gal}}$ relation at high redshift becomes very steep (see Figure 8 below), and

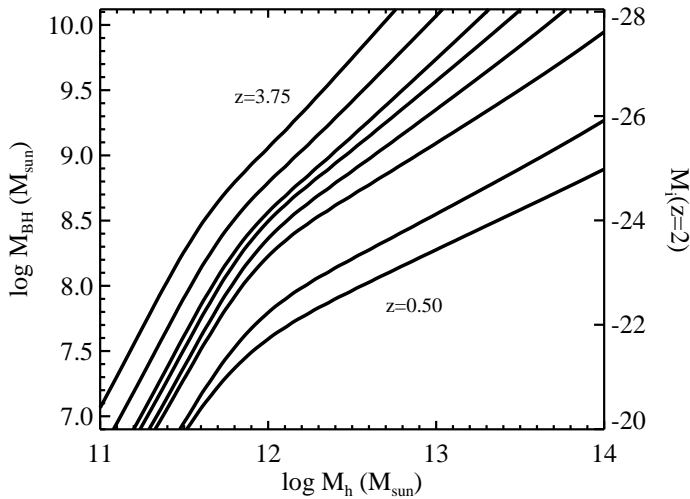


Figure 8. The typical black hole mass in the central galaxy of a halo of mass M_h , vs. M_h , for a number of redshifts (corresponding to the redshifts shown in Figure 3). The typical BH mass corresponding to a fixed M_h increases with z , as expected. Note the significant curvature in the relation, which arises due to our assumption that galaxy properties regulate the size of black holes and the well-known inefficiencies of galaxy formation in high and low halo masses. Since the x -axis controls the clustering amplitude while the y -axis controls the observed luminosity, the curvature of this relation has important implications for the luminosity dependence of quasar clustering (see §3.2).

so even a significant change in α or η changes the clustering only modestly. Similarly, changes in the assumed $L_Q - M_{\text{BH}}$ scatter within the range 0.3–0.6 dex does not significantly alter the predicted clustering. This occurs because a change in scatter induces a change in α that happens to leave the clustering essentially unchanged. Future constraints on the clustering of high-redshift quasars will place strong constraints on this model, as discussed further in §4.1, and may indicate that some of our model assumptions break down as we approach an era of rapid BH growth at high z .

Observationally, it has proven very difficult to measure a dependence of clustering strength on quasar luminosity (see e.g., Shen et al. 2009, for a recent example), in part because the significant scatter between quasar luminosity and halo mass will dilute any intrinsic relation between clustering strength and luminosity. We address this issue in Figure 7, where we plot the large-scale bias as a function of luminosity and redshift. Here the model bias was computed via the relation between bias, halo mass, and cosmology from Tinker et al. (2010).

We find a very shallow relation between bias and quasar luminosity below $M_i(z=2) \sim -26$. In our model this occurs for three reasons: (1) the intrinsic relation between bias and halo mass is very shallow below the characteristic halo mass, which at $z \sim 0$ is $\sim 10^{13} M_\odot$; (2) the $M_{\text{BH}} - M_h$ relation becomes very steep at low mass, implying that a large range in quasar luminosities maps into a small range in halo masses; (3) scatter in the $M_{\text{gal}} - M_h$, $M_{\text{BH}} - M_{\text{gal}}$, and $L_Q - M_{\text{BH}}$ relations acts to dilute the strong clustering in high mass halos. The degree of luminosity dependence (as well as the absolute value of the bias) is sensitive to the scatter in the $L_Q - M_h$ relation, with more scatter leading to less L -dependence. This weak luminosity-dependent clustering is also predicted in the models of Croton (2009), Shen (2009), and Hopkins et al. (2008).

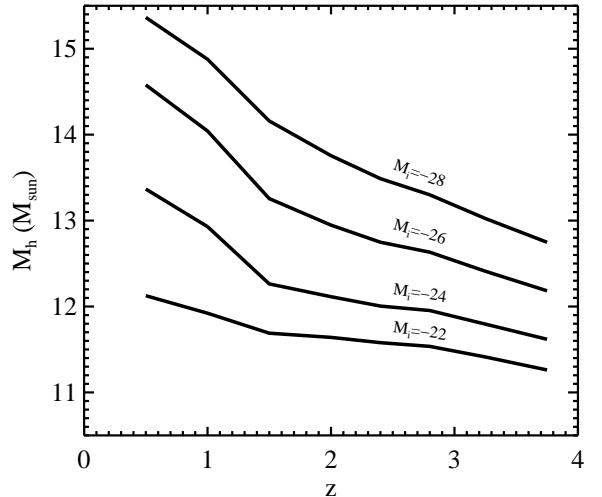


Figure 9. Relation between halo mass and redshift for quasars of a fixed luminosity. At low redshift the range of halo masses hosting quasars is very broad, but the distribution narrows substantially at high redshift. This is simply a recasting of the relations shown in Figure 8.

Figure 7 demonstrates that we expect significant luminosity dependent quasar bias only for very luminous quasars. However, measuring the autocorrelation function of such luminous quasars is made difficult by their low space densities, which can be illustrated as follows. The error on the bias in the high- L regime is dominated by counting statistics. The number of pairs within e.g., 20Mpc is $(1/2)\bar{n}_Q^2 [1 + \bar{\xi}_{20}] V_{\text{survey}} V_{20}$ where $V_{20} = (4\pi/3)(20\text{Mpc})^3$, V_{survey} is the survey volume, \bar{n}_Q is the quasar space density, and $\bar{\xi}$ is the volume average correlation function. For $\xi(r) = (r_0/r)^2$ we have $\bar{\xi} = 3\xi$, and $r_0 \sim 10 - 20 h^{-1}\text{Mpc}$ so we expect $\bar{\xi} \sim \mathcal{O}(1)$. One hundred pairs within 20Mpc would return an error on the bias of $\sim 10\%$, and for a fiducial survey volume of 10^{10}Mpc^3 , this corresponds to a quasar number density of $\approx 5 \times 10^{-7}\text{Mpc}^{-3}$. The luminosity corresponding to this number density at each redshift is marked by a solid symbol along the $b(L)$ relation in Figure 7. In order to probe the bias for quasars at higher luminosities it will be necessary to resort to cross-correlation techniques, which allow estimates of the bias of objects with extremely low space density. An appealing method would be to cross-correlate existing spectroscopic samples of quasars with samples of galaxies or lower luminosity quasars selected from deeper photometry in upcoming surveys such as DES, Pan-STARRS, SUMIRE and LSST.

Finally, we emphasize that there are several model parameters that were assumed herein that affect the clustering of quasars. In particular, the scatter between L_Q , M_{gal} and M_h has a significant effect on the luminosity-dependence of bias. As mentioned previously, the Eddington ratio, η , is perfectly degenerate with α , and so with the freedom to vary the normalization in the $M_{\text{BH}} - M_{\text{gal}}$ relation, the clustering will be insensitive to η . Seen another way, constraints on α from observations will in turn allow a constraint on η within the context of our model.

4. DISCUSSION

4.1. Implications

The success of our model in reproducing the basic demographics of quasars allows us to consider several implications that follow naturally within our framework.

In Figure 8 we show the best-fit model $M_h - M_{\text{BH}}$ relations from $z = 0.5$ to $z = 3.75$ (the model at $z = 4.75$ is highly under-constrained and so is not plotted). As discussed above, the quasar LF places very weak constraints on the model relations at $\log(M_h/M_\odot) > 13.5$, and so one should interpret the model relations in Figure 8 with this in mind. It is also worth pointing out that while the model formally allows for the existence of extremely massive BHs with $M_{\text{BH}} > 10^{10} M_\odot$ residing within moderately massive halos, at high redshift such halos are very rare. For example, at $z = 4.75$ one expects only of order one halo with $\log(M_h/M_\odot) > 13$ per 10^9 Mpc^3 .

In the model, lower mass black holes are growing to lower redshift faster than higher mass black holes (this is sometimes referred to as downsizing). In fact, a strict interpretation of the results has the disconcerting property that the BHs in the most massive galaxies lose mass below $z \approx 2$. This arises directly from two observational facts: (1) $M_{\text{BH}}/M_{\text{gal}}$ declines with time as $(1+z)^2$ (McLure et al. 2006; Targett, Dunlop & McLure 2012) and (2) the most massive galaxies grow very little between $z \approx 2$ and the present, at least within the inner several kpc where high-redshift galaxies are typically photometered (e.g., Pérez-González et al. 2008; Marchesini et al. 2009; van Dokkum et al. 2010). There are several caveats worth noting in this context. First, the slope of the $M_{\text{BH}} - M_{\text{gal}}$ relation is not well-known at high M_{gal} , owing largely to the rarity of such objects. Second, the difficulty in measuring the total light from galaxies implies that non-trivial systematic uncertainties still plague conclusions regarding the evolution of the most massive galaxies from $0 < z < 2$. Finally, as demonstrated in Figure 5, the model is essentially unconstrained at the highest masses, and so any conclusions regarding evolution at the high-mass end must be treated with caution. Evolution in Eddington ratios (advocated by Shen & Kelly 2012), curvature in the scaling relations or strong evolution in bulge-to-total mass ratio could all play a role in alleviating the tension. Future observations of the evolution of the $M_{\text{BH}} - M_{\text{gal}}$ relation at high mass will be necessary to make further progress.

Figure 9 shows the evolution of the halo mass for quasars of fixed luminosity. The trend of lower M_h at higher z was already apparent in Figure 8. Figure 9 also emphasizes how the range of halo masses for a fixed luminosity range narrows towards higher z . This effect is in the opposite sense to models which tie the luminosity of quasars directly to halo properties (e.g. Croton 2009). Our model is able to reproduce the observed L -independent clustering at low z because the run of bias with halo mass also becomes shallower at low z for the halo masses of interest.

Figure 10 shows the evolution of the quasar luminosity function as predicted by our model once the parameters are fit to the available data. The evolution of the LF is driven by evolution in the $M_{\text{BH}} - M_{\text{gal}}$ and $M_{\text{gal}} - M_h$ relations and the evolution of the halo mass function (the $L_Q - M_{\text{BH}}$ relation does not evolve in our fiducial model). The break in the model quasar LF arises primarily due to the shape of the $M_{\text{gal}} - M_h$ relation, and thus L_* quasars live in halos near the peak of that relation, $M_h \sim 10^{12} M_\odot$. The peak of the $M_{\text{gal}} - M_h$ relation changes

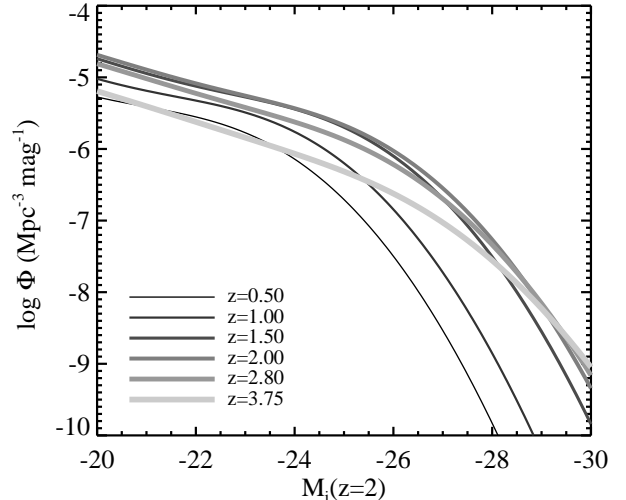


Figure 10. The best-fit quasar luminosity function for a variety of redshifts. Notice the rapid drop in the LF at high luminosity at $z < 2$, which, in our model, is largely responsible for the rapid drop in the cosmic quasar number density at late times. The break in the quasar LF scales approximately as $(1+z)^2$; see the text for details.

very little with redshift (Behroozi, Wechsler & Conroy 2012, e.g.), so that at fixed M_h there is little change of M_{gal} with z . However the luminosity of the break can evolve due to a combination of evolution in the $M_{\text{BH}} - M_{\text{gal}}$ relation or the Eddington ratio. In our fiducial model η is constant and $M_{\text{BH}} \propto (1+z)^2$ at fixed M_{gal} and so the break in the luminosity function scales as $(1+z)^2$. The faint-end slope of the model LF does not vary significantly, in good agreement with the data, and the overall normalization changes only modestly. The major departure from pure luminosity evolution is the change in the slope of the bright end. The bright-end slope appears shallower at higher z both because the data are probing closer to the (brighter) break of the LF and because the $M_{\text{BH}} - M_h$ relation becomes steeper at higher mass and redshift. We also note that the bright end of the model LF is strongly suppressed at $z < 1.5$, and it is this suppression that is responsible for much of the drop in the quasar number density to lower redshift. The drop is a consequence of the shallowing of the $M_{\text{BH}} - M_h$ relation at high mass, which is in turn driven by the very slow growth of massive galaxies at low redshift.

In fact, the model naturally reproduces the global rise and fall of the quasar number density over the interval $0.5 < z < 4.75$. This follows simply from the evolution in the $M_{\text{gal}} - M_h$ and $M_{\text{BH}} - M_{\text{gal}}$ relations and the halo mass function; it does not require strong evolution in t_Q at low z . Specifically we do not invoke a decline in the cold gas fraction nor a decline in the major merger rate at $z < 2$ in order to reproduce the observed decline in the abundance of quasars. While these physical processes may ultimately be responsible for shaping the evolving relations between M_{BH} , M_{gal} and M_h , they do not appear explicitly in the model.

Our model suggests a very different picture of how quasars inhabit massive halos compared to previous work. Rather than having a preferred halo mass scale (around $10^{12} M_\odot$) for quasar activity we have actively accreting black holes in a broad range of galaxy and halo masses. The apparent preference for quasars to live in halos of $10^{12} M_\odot$ arises from

the shape of the $M_{\text{gal}} - M_h$ relation, which reflects the well known fact that galaxy formation is most efficient in halos near $10^{12} M_{\odot}$, along with the shape of the halo mass function.

Due to its simplicity the model predicts the clustering of any population of quasars once the two model parameters are fixed (e.g., by the observed LF). Variation in the $L_Q - M_h$ scatter or $M_{\text{BH}} - M_{\text{gal}}$ slope do not strongly affect the predicted clustering, meaning that our model makes an essentially parameter-free prediction of the clustering of quasars as a function of luminosity and redshift. Overall the agreement between the predicted clustering and the observations is good, though there is a tendency for the model to slightly underpredict the observations and there is some tension at the highest redshifts. This tension has been noted before – the very high amplitude of clustering measured at $z \sim 4$, in combination with the abundance, requires quasars to have a duty cycle approaching unity and almost no scatter in L_Q at fixed M_h (White, Martini & Cohn 2008; Shankar, Weinberg & Shen 2010). If these measurements can be strengthened, possibly by cross-correlation of existing spectroscopic quasar samples with deeper photometric quasar or galaxy samples, then it will indicate that one of our assumptions is breaking down as we approach the era of rapid black hole growth in the early Universe.

We make no assumption about what triggers quasar activity, whether it be a major merger of two gas rich galaxies, a secular instability in a disk, or a critical halo mass. In general it is quite difficult to translate abundance and clustering measurements into constraints on the underlying mechanisms that trigger quasar activity. We can gain some insight by the fact that our duty cycle, or quasar lifetime, is relatively independent of redshift with a tendency to fall towards higher redshifts rather than rise. If quasars are visible for a fixed, but short, time and are triggered by mergers then we expect t_Q to scale with the merger rate (c.f. Carlberg 1990). The merger rate for halos, per halo, per unit redshift is relatively flat (Lacey & Cole 1993; Percival et al. 2003; Cohn & White 2005; Wetzel, Cohn & White 2009; Fakhouri & Ma 2009; Hopkins et al. 2010b), so if we can naively translate halo mergers into galaxy mergers we expect a rate (per unit time) scaling as $(1+z)H(z) \propto (1+z)^{5/2}$ for $z \gg 1$. If quasars are visible for a constant interval after each merger then $t_Q \propto 1+z$, which is not in good agreement with our best-fit relation. Of course, galaxy merger rates can differ from halo merger rates. A recent analysis by Hopkins et al. (2010a) suggests a rate per unit time scaling as $(1+z)^{1.5-2.0}$, which would lead to slower evolution in t_Q , as we observe. Such agreement is not conclusive however, and we cannot rule out secular processes or a time-varying combination of multiple triggers.

4.2. Comparison to Previous Work

The success of our model in explaining the basic demographics of quasars with relatively few, smoothly varying inputs goes a long way to explaining the manner in which forward modeling of the quasar population can succeed with relatively little fine tuning. Both semi-analytic models (e.g., Cattaneo, Haehnelt & Rees 1999; Kauffmann & Haehnelt 2000, 2002; Volonteri, Haardt & Madau 2003; Bromley, Somerville & Fabian 2004; Granato et al. 2004; Croton et al. 2006; Monaco, Fontanot & Taffoni 2007; Malbon et al. 2007; Bonoli et al. 2009; Fanidakis et al. 2012; Hirschmann et al. 2012) and hydrodynamic simulations (e.g., Sijacki et al. 2007; De Graf et al. 2011) adjust their subgrid

models to ensure a reasonable match to the $M_{\text{gal}} - M_h$ relation over a broad redshift range, thus ensuring that galaxies populate halos in approximately the correct manner. All of the models introduce a $M_{\text{BH}} - M_{\text{gal}}$ relation through either or a combination of common feeding mechanisms and feedback-limited BH growth. As we have shown, with these two ingredients even simple lightcurve models are sufficient to match the basic demographics of quasars over a broad range of luminosity and redshift. A good match to the data can be found for a wide range of scatter in $M_{\text{BH}} - M_{\text{gal}}$, or evolution in the scatter. Conversely, if a model has difficulties reproducing the stellar mass function and its evolution then it will need to incorporate mass-dependent quasar physics that counteracts this deficiency in order to match the observed quasar properties.

By contrast, models that tie black hole properties directly to the underlying halo population need to introduce more complexity in order to reproduce the observed properties of quasars. Recent examples include Lidz et al. (2006), Croton (2009), and Shen (2009), who all need to include mass- and redshift-dependent duty cycles to explain the shape and evolution of the quasar luminosity function. While our model and theirs can produce qualitatively similar fits to the basic data, the explanations for the observed behaviors differ. One of the most basic differences is the range of halos that host active quasars, and its evolution (discussed above). This in turn affects how each model explains the evolution of the quasar LF and the luminosity-independence of quasar clustering.

Conventional wisdom is that the quasar duty cycle is required by the data to be a (strong) function of luminosity (e.g. Adelberger & Steidel 2005; Hopkins et al. 2005; Lidz et al. 2006; Croton 2009; Shen 2009). In our model this is not the case. There are two major reasons for this. The first is that we obtain a flattening of the $b(L)$ relation from the steepness of the $L_Q - M_h$ relation at low L_Q and second is the intrinsic scatter³ in that relation. Thus our model is not a “light bulb” model in the sense of Hopkins et al. (2005); Lidz et al. (2006), who reserve that term for a model in which there is no scatter in $L_Q - M_h$. However scatter in the $L_Q - M_h$ relation is *expected*, due to the observed scatter in $M_{\text{BH}} - M_{\text{gal}}$ and variation in Eddington ratios if from no other source; for this reason we refer to our model as a “scattered” light bulb model. This expected level of scatter is enough to make $b(L)$ flat until extremely high L or correspondingly low \bar{n}_Q (a similar behavior is seen in the model of Croton 2009, which is also not strictly a light bulb model in the above sense). For this reason we are able to obtain a model in which both the quasar lifetime and the quasar clustering are independent of L .

Aird et al. (2012) studied X-ray selected active galactic nuclei (AGN) as a function of galaxy mass at $z \sim 0.6$ and found no preference for AGN to be found in galaxies of a particular mass at fixed Eddington ratio, even for ratios as high as $\eta \gtrsim 0.1$. Their results suggest a duty cycle that does not depend strongly on galaxy mass, in excellent agreement with our results.

Finally, the apparent preference for quasars to live in halos of $10^{12} M_{\odot}$, which has been noted by many authors, arises in our model from the shape of the $M_{\text{gal}} - M_h$ relation which reflects the well-known fact that galaxy formation is most ef-

³ This scatter may arise due to time-dependent processes, i.e. a high L_Q object at the time of observation is not required to have always been or continue to be high L_Q .

efficient in halos of $10^{12}M_{\odot}$. Within the context of our model this cannot be taken as evidence for a merger driven origin to quasar activity, despite the fact that it is close to the small group scale where mergers may be more efficient, because it is not believed that the peak of the $M_{\text{gal}} - M_h$ relation at this scale is related to mergers.

4.3. Mock Catalogs

While our intent has been to understand the quasar phenomenon, the model can also be used for the creation of mock catalogs from N-body simulations. The simplicity of the model makes it easy to rapidly generate redshift-dependent quasar populations that have the correct luminosity function and clustering, given halo catalogs at the redshifts of interest. The steps for creating such a catalog are straightforward:

1. Adopt the redshift-dependent $M_{\text{gal}} - M_h$ relation from Behroozi, Wechsler & Conroy (2012), including scatter in M_{gal} at fixed M_h .
2. Use the $M_{\text{gal}} - M_{\text{BH}}$ relation from Equation 1 to assign BHs to galaxies, including 0.3 dex of scatter in M_{BH} at fixed M_{gal} . As our best-fit normalization is close to the McLure et al. (2006) relation, especially at $z < 3$, we suggest fixing $\alpha = -3.1$ in this equation.
3. Randomly turn a fraction, f_{on} , of the BHs into active quasars. As evident from Figure 4, the quasar lifetime is approximately constant at 3×10^7 yr at $z < 3$; we therefore advocate fixing t_Q to this value. One then determines the duty cycle via $f_{\text{on}}(z) = t_Q/t_H(z)$.
4. For the active BHs, convert M_{BH} into L_Q using Equation 2, with an additional 0.3 dex of scatter in L_Q at fixed M_{BH} .

When simulations are populated with quasars in this way, the mock quasar LF and clustering will agree with all existing LF and clustering data at $z < 3$. In order to produce mock catalogs at higher redshifts one will need to include a drop in t_Q as shown in Figure 4. Such mock catalogs should prove useful in the context of ongoing and future planned surveys such as BOSS, bigBOSS, DES, Pan-STARRS, SUMIRE and LSST.

5. SUMMARY

We have presented a simple model for quasars with the aim of understanding to what extent their demographics arise naturally from what is known about the evolution of galaxies along with plausible assumptions about how black holes inhabit them. The key feature of the model is that the properties of black holes are set by those of their host galaxies rather than their host halos (see also White et al. 2012). In the model, BH mass is linearly related to galaxy mass and BHs shine at a fixed fraction of the Eddington luminosity during accretion episodes. Galaxies are related to dark matter halos via empirically constrained relations (Behroozi, Wechsler & Conroy 2012). The model has only two free parameters at each redshift, the normalization of the $M_{\text{BH}} - M_{\text{gal}}$ relation and the duty cycle, both of which are tightly constrained by observations of the quasar LF. The model provides an excellent fit to the LF data for $0.5 < z < 5$ and reproduces the observed clustering at intermediate redshifts with no additional adjustable parameters.

The best-fit model parameters have $M_{\text{BH}}/M_{\text{gal}} \propto (1+z)^2$, as observed, and a quasar lifetime of approximately 10^7 yr independent of epoch. This may be expected if the growth of the galaxy during a quasar event only allows ~ 1 e-folding of black hole growth before feedback halts quasar activity.

There are several implications of our model, which we now summarize:

- Actively accreting BHs are equally likely to exist in galaxies, and dark matter halos, over a wide range in masses. The BHs in halos more massive than $10^{13.5}M_{\odot}$ contribute very little to the observed quasar LF at any redshift due to their rarity. The quasar LF therefore places weak constraints on the quasar duty cycle in massive halos.
- The break in the quasar LF is a reflection of the peak in the $M_{\text{gal}} - M_h$ relation at $M_h \sim 10^{12}M_{\odot}$ and the observed evolution of the LF primarily reflects the $(1+z)^2$ scaling of L_Q/M_{gal} and the change in shape of the $M_{\text{gal}} - M_h$ relation. The bright-end slope of the quasar LF appears shallower at high z both because the data are probing closer to the (brighter) break in the LF and because the $M_{\text{BH}} - M_h$ relation becomes steeper at higher mass and redshift.
- Our model naturally reproduces the global rise and fall of the quasar number density over the interval $0.5 < z < 5$. This follows simply from the evolution in the $L_Q - M_h$ relation and does not require strong evolution in the quasar lifetime. The bright end of the model quasar LF is strongly suppressed at $z < 1.5$, due to the slow growth of massive galaxies, and this is responsible for much of the drop in quasar number density to low redshift.
- The apparent preference for quasars to live in halos of $10^{12}M_{\odot}$ arises from the shape of the $M_{\text{gal}} - M_h$ relation, which reflects the well-known fact that galaxy formation is most efficient near $10^{12}M_{\odot}$, in conjunction with the steepness of the halo mass function at high mass.
- There is some tension between our model and the amplitude of clustering observed at $z \sim 4$; the latter, taken at face value, suggests that quasars have a duty cycle approaching unity and almost no scatter in $L_Q - M_h$. Future measurements in this redshift range will be crucial tests of the model.
- The nearly constant inferred quasar lifetimes as a function of luminosity and redshift should provide valuable constraints on the triggering mechanisms for quasars.

Measurements of quasar demographics at higher redshifts and lower luminosities will help to further constrain and test our model. In particular, stronger constraints on the quasar LF at $z > 4$, quasar clustering as a function of luminosity and redshift, and the $M_{\text{BH}} - M_{\text{gal}}$ relation as a function of redshift, will provide very strong constraints on the model parameters. Moreover, with such observational constraints in hand, we will be able to directly constrain the mean Eddington ratio as a function of redshift and the scatter as a function of redshift, providing further insight into the link between quasars, galaxies, and dark matter halos.

We thank Nic Ross and Yue Shen for providing their clustering data in electronic form, and Adam Myers, Matt McQuinn, and Yue Shen for comments on an earlier draft. M.W. was supported by the NSF and NASA. This work made extensive use of the NASA Astrophysics Data System and of the `astro-ph` preprint archive at `arXiv.org`. The analysis made use of the computing resources of the National Energy Research Scientific Computing Center.

REFERENCES

- Adelberger K. L. & Steidel C. C., 2005, *ApJ*, 630, 50
Aird J., et al., 2012, *ApJ*, 746, 90
Alexander D.M., Hickox R.C., 2012, to appear in *New Astronomy Reviews* [arXiv:1112.1949]
Behroozi P.S., Wechsler R.H., Conroy C., 2012, preprint [arXiv:1207.6105]
Bonoli S., Marulli F., Springel V., White S.D.M., Branchini E., Moscardini L., 2009, *MNRAS*, 396, 423
Booth C.M., Schaye J., 2010, *MNRAS*, 405, L1
Bromley J.M., Somerville R.S., Fabian A.C., 2004, *MNRAS*, 350, 456
Bryan, G. L. and Norman, M. L., 1998, *ApJ*, 495, 80
Carlberg R.G., 1990, *ApJ*, 350, 505
Cattaneo A., Haehnelt M.G., Rees M.J., 1999, *MNRAS*, 308, 77
Chabrier, G., 2003, *PASP*, 115, 763
Ciotti L., Ostriker J.P., 1997, *ApJ*, 487, 105
Ciotti L., Ostriker J.P., 2001, *ApJ*, 551, 131
Cohn J.D., White M., 2005, *Astroparticle Physics*, 24, 316
Conroy C., Wechsler R.H., 2009, *ApJ*, 696, 620
Croom S.M., et al., 2004, *MNRAS*, 349, 1397
Croom S.M., et al., 2009, *MNRAS*, 392, 19
Croton D.J., et al., 2006, *MNRAS*, 365, 11
Croton D.J., 2009, *MNRAS*, 394, 1109
Davis M., Efstathiou G., Frenk C.S., White S.D.M., 1985, *ApJ*, 292, 371
Decarli R., Falomo R., Treves A., Labita M., Kotilainen J.K., Scarpa R., 2010, *MNRAS*, 402, 2453
Efstathiou G., Rees M.J., 1988, *MNRAS* 230, 5
Fakhouri O., Ma C.-P., 2009, *MNRAS*, 394, 1825
Fanidakis N., Baugh C.M., Benson A.J., Bower R.G., Cole S., Done C., Frenk C.S., Hickox R.C., Lacey C., del P. Lagos C., 2012, *MNRAS*, 419, 2797
De Graf C., Di Matteo T., Khandai N., Croft R., Lopez J., Springel V., 2011, preprint [arXiv:1107.1254]
Glikman, E., Bogosavljević M., Djorgovski S.G., Stern D., Dey A., Jannuzi B.T., Mahabal A., 2010, *ApJ*, 710, 1498
Granato G.L., de Zotti G., Silva L., Bressan A., Luigi D., 2004, *ApJ*, 600, 580
Haiman Z., Ciotti L., Ostriker J.P., 2004, *ApJ*, 606, 763
Haiman Z., Loeb A., 1998, *ApJ*, 503, 505
Haring N., Rix H., 2004, *ApJ*, 604, L89
Hirschmann M., Somerville R. S., Naab T., Burkert A., *MNRAS* submitted [arXiv:1206.6112]
Hopkins P.F., Somerville R.S., Hernquist L., Cox T.J., Robertson B., Li Y., 2006, *ApJ*, 652, 864
Hopkins P., Hernquist L., Cox T.J., Di Matteo, T., Robertson, B., Springel, V. 2005, *ApJ*, 630, 716
Hopkins P., Hernquist L., Cox T.J., Robertson B., Krause E., 2007a, *ApJ*, 669, 45.
Hopkins P., Hernquist L., Cox T.J., Robertson B., Krause E., 2007b, *ApJ*, 669, 67
Hopkins P.F., Hernquist L., Cox T.J., Keres D., 2008, *ApJS*, 175, 356
Hopkins P., et al., 2010a, *ApJ*, 715, 202
Hopkins P., et al., 2010b, *ApJ*, 724, 915
Kauffmann G., Haehnelt M., 2000, *MNRAS*, 311, 576
Kauffmann G., Haehnelt M., 2002, *MNRAS*, 332, 529
King A., 2003, *ApJL*, 596, L27
Kollmeier J.A., et al., 2006, *ApJ*, 648, 128
Kormendy J., Richstone D., 1995, *ARA&A*, 33, 581
Lacey C., Cole S., 1993, *MNRAS*, 262, 627
Lidz A., Hopkins P.F., Cox T.J., Hernquist L., Robertson B., 2006, *ApJ*, 641, 41.
Lynden-Bell D., 1969, *Nature*, 223, 690
Malbon R.K., Baugh C.M., Frenk C.S., Lacey C.G., 2007, *MNRAS*, 382, 1394
Mandelbaum, R. and Seljak, U. and Kauffmann, G. and Hirata, C. M. and Brinkmann, J., 2006, *MNRAS*, 344, 847
Marchesini D., et al., 2009, *ApJ*, 701, 1765
Martini P., 2004, “QSO lifetimes”, in “Coevolution of Black Holes and Galaxies”, from the Carnegie Observatories Centennial Symposia, Carnegie Observatories Astrophysics Series. Ed. L.C.Ho, p. 169 (Cambridge University Press)
Marulli F., Crociani D., Volonteri M., Branchini E., Moscardini L., 2006, *MNRAS*, 368, 1269
Masters, D. et al., 2012, *ApJ* in press [arxiv:1207:2154]
Di Matteo T., Khandai N., DeGraf C., Feng Y., Croft R.A.C., Lopez J., Springel V., 2012, *ApJ*, 745, L29
McLure, R.J., Jarvis M.J., Targett T.A., Dunlop J.S., Best P.N., 2006, *NewAR*, 50, 782
Merloni A., et al., 2010, *ApJ*, 708, 137
Monaco P., Fontanot F., Taffoni G., 2007, *MNRAS*, 375, 1189
Moster B., et al., 2010, *ApJ*, 710, 903
Natarajan P., 2012, in “Proceedings of the XVth Congress of Philosophy & Foundations of Science”, to be published by the American Institute of Physics [arXiv:1105.4902]
Peng C.Y., Impey C.D., Rix H-W., Falco E.E., Keeton C., Kochanek C.S., Lehar J., McLeod B.A., 2006, *NewAR*, 50, 689
Pérez-González P.G., et al., 2008, *ApJ*, 675, 234
Percival W.J., Scott D., Peacock J.A., Dunlop J.S., 2003, *MNRAS*, 338, L31
Richards G.T., et al., 2006, *AJ*, 131, 2766
Ross N.P., et al., 2009, *ApJ*, 697, 1634
Salpeter, E.E., 1964, *ApJ*, 140, 796
Shankar F., 2009, *New AR*, 53, 57
Shankar F., Weinberg D.H., Shen Y., 2010, *MNRAS*, 406, 1959
Shen Y., et al., 2008, *ApJ*, 680, 169
Shen Y., 2009, *ApJ*, 704, 89
Shen Y., et al., 2009, *ApJ*, 697, 1656
Shen Y., Kelly B.C., 2012, *ApJ*, 746, 169
Shlosman I., Frank J., Begelman M.C., 1989, *Nature*, 338, 45
Sijacki D., Springel V., Di Matteo T., Hernquist L., 2007, *MNRAS* 380, 877
Silk J., Rees M.J., 1998, *A&A*, 331, L1
Springel V., Di Matteo T., Hernquist L., 2005, *MNRAS*, 361, 776
Targett T.A., Dunlop J.S., McLure R., 2012, *MNRAS*, 420, 3621
Tinker J., et al., 2008, *ApJ*, 688, 709
Tinker J., et al., 2010, *ApJ*, 724, 878
Trainor R.F., Steidel C.C., 2012, *ApJ*, 752, 39
Tremaine S., et al., 2002, *MNRAS*, 574, 740
Trujillo-Gomez S., Klypin A. Primack J., Romanowsky A.J., 2011, *ApJ*, 742, 16
Vale A., Ostriker J.P., 2004, *MNRAS*, 353, 189
van Dokkum P.G., et al., 2010, *ApJ*, 709, 1018
van den Bosch, F. C., Yang X., Mo H.J., 2007, *MNRAS*, 340, 771
Volonteri M., Haardt F., Madau P., 2003, *ApJ*, 582, 559
Wetzel A., Cohn J.D., White M., 2009, *MNRAS*, 394, 2182
White M., 2002, *ApJS*, 579, 16
White M., Martini P., Cohn J.D., 2008, *MNRAS*, 390, 1179
White M., et al., 2012, *MNRAS*, 424, 933
Wolf C., Wisotzki L., Borsch A., Dye S., Kleinheinrich M., Meisenheimer K., 2003, *A&A*, 408, 499
Wyithe J.S.B., Loeb A., 2002, *ApJ*, 581, 886
Wyithe J.S.B., Loeb A., 2003, *ApJ*, 595, 614